ENSEMBLES

Climate change and its impacts

at seasonal, decadal and centennial timescales

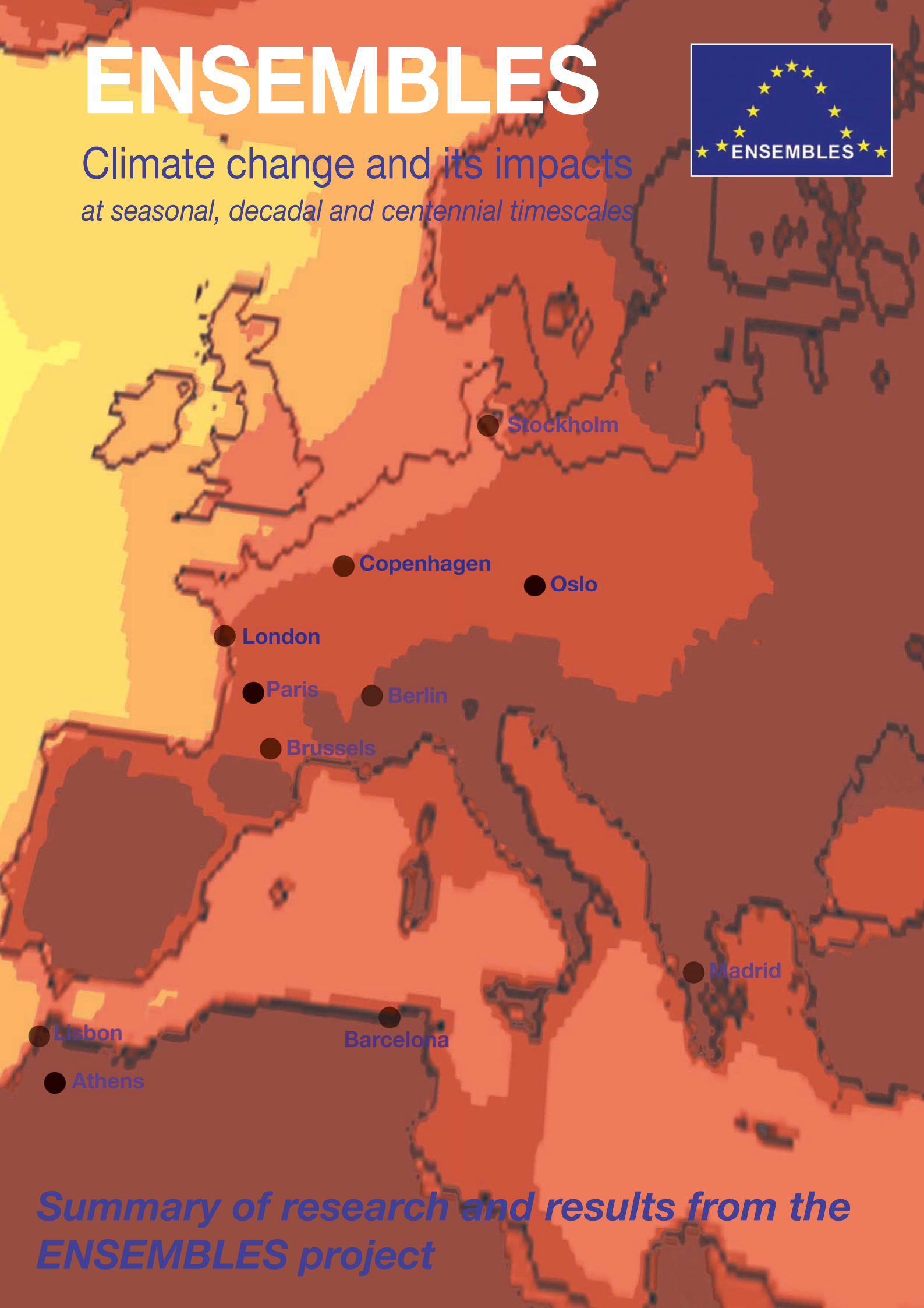

Summary of research and results from the ENSEMBLES project

Project and Contact Information

ENSEMBLES is an integrated research project running from 2004 to 2009 and is coordinated by the Met Office Hadley Centre. It has produced probabilistic projections of climate for Europe to help inform researchers, decision makers, businesses and the public with climate information from the latest climate modelling and analysis tools.

ENSEMBLES is funded by the European Commission under the 6th Framework Programme Priority: Global Change and Ecosystems.

This report summarises the science research and results of the ENSEMBLES project. For more information please see *www.ensembles-eu.org* or contact us using the details below:

ENSEMBLES project office
Met Office Hadley Centre, FitzRoy Road, Exeter EX1 3PB, UK

Paul van der Linden
ENSEMBLES Director
+44 1392 884163
paul.vanderlinden@metoffice.gov.uk

Prof John F.B. Mitchell
ENSEMBLES Coordinator
+44 1392 884604
john.f.mitchell@metoffice.gov.uk

Pip Gilbert
ENSEMBLES Secretary
+44 1392 884603
ensemblesfp6@metoffice.gov.uk

European Commission
Climate Change and Environmental Risks Unit, General Directorate for Research, European Commission, CDMA 3/006, B-1049 Brussels, Belgium

Dr Philippe Tulkens
EC Project Officer
philippe.tulkens@ec.europa.eu

Editors
Paul van der Linden and John F.B. Mitchell of the Met Office Hadley Centre, FitzRoy Road, Exeter EX1 3PB, UK

Citation
Sections can be referenced by their title and authors, if citing the whole report please use:
van der Linden P., and J.F.B. Mitchell (eds.) 2009: ENSEMBLES: Climate Change and its Impacts: Summary of research and results from the ENSEMBLES project. Met Office Hadley Centre, FitzRoy Road, Exeter EX1 3PB, UK. 160pp.

Contract number: GOCE-CT-2003-505539
Website: http://www.ensembles-eu.org
Project duration: 1 September 2004 to 31 December 2009
Full list of project partners is given on page 158

Credit and caption for cover picture:
The front cover of this report shows some European cities relocated to places where the current climate is the same as what the projected climate will be for that city in 2071–2100. The methodology involves running a multi-model ensemble of Regional Climate Models out to 2100 against a 1961–1990 climatological baseline and comparing the city climates between the two periods. The comparison takes into account temperature, precipitation and seasonal characteristics for each city. The cities are superimposed on a background of temperature anomaly for the 2071–2100 period of the ENSEMBLES multi-model average for Europe, Figure A1.13. Thanks go to the following people:
Stephane Hallegatte, Météo-France and CIRED, for developing the technique and producing the map,
Else van den Besselaar, KNMI, for providing the observed climate data,
Ole Christensen, DMI, for providing the temperature and rainfall projections for the end of the century.

8 Evaluation of the ENSEMBLES Prediction System

[Research Theme 5]

A.M.G. Klein Tank (KNMI), E. Manzini (INGV), P. Braconnot (IPSL), F. Doblas-Reyes (ECMWF), T.A. Buishand (KNMI), A. Morse (Liverpool University)

8.1 Introduction

To assess the quality of the ensemble prediction system for climate change, a comprehensive and independent evaluation was performed against analyses/observations. The evaluation included seasonal to decadal as well as climate change time-scales and all spatial scales. The focus has been on:

- the representation of key phenomena and processes causing variability in Global Climate Model (GCM) simulations;
- the actual and potential seasonal to decadal forecast quality;
- the amount of change in the occurrence of extremes in Regional Climate Model (RCM) simulations compared with gridded observational data;
- the quality of impact models when forced with downscaled reanalysis data and hindcasts.

To facilitate this work, a new, quality-controlled and high-resolution, gridded observational dataset for Europe was developed as part of the project.

8.2 Relevance to decision makers

The quality of the probabilistic predictions by the ensemble prediction system depends critically on the ability of the Global and Regional Climate Models to simulate key processes and to reproduce the statistics of present-day weather and climate variability. For impact studies and adaptation strategies in European countries, in particular the representation of extremes in Regional Climate Models, is important. But high-resolution regional modelling only makes sense if the global models that provide the boundaries for the regional models have sufficient quality. The comparison of GCM and RCM simulations against observations, as performed in this Research Theme, provides insights into the extent that climate models can be used for climate prediction. The evaluation also helps in assessing the uncertainties in the response of models to anthropogenic forcing.

8.3 The E-OBS daily gridded dataset for Europe

A new daily observational dataset has been developed for surface climate variables. The dataset covers Europe, for the greater part with a resolution high enough to capture extreme weather and climate events. The dataset includes associated information on uncertainty due to sampling and interpolation.

The ENSEMBLES gridded observational dataset (E-OBS) is a European land-only daily high-resolution dataset for precipitation and minimum, mean and maximum surface temperature for the period from 1950 to the present. This dataset improves on other products in its spatial resolution and extent, time period, number of contributing stations, and research into finding the most appropriate method for spatial interpolation of daily climate observations (Hofstra et al., 2008). A full description can be found in Haylock et al. (2008). The underlying station data are from the quality-controlled daily observations of the European Climate Assessment and Dataset project (ECA&D – http://eca.knmi.nl; see Klok and Klein Tank, 2008).

The E-OBS dataset is publicly available from http://eca.knmi.nl/ensembles, strictly for use in non-commercial research and non-commercial education projects only. The gridded dataset is made available on two regular latitude–longitude grids (resolutions 0.25 and 0.50 degrees) and on two rotated pole grids (resolutions 0.22 and 0.44 degrees) with the North Pole at 39.25 N, 162 W. It covers the area between 25 N to 75 N and 40 W to 75 E. The regular grid is the same as that for the monthly datasets available from the Climatic Research Unit (CRU) and the rotated grid is the same as that used in many ENSEMBLES Regional Climate Models (RCMs). The interpolation method has been designed to provide the best estimate of grid-box averages rather than point values. This enables direct comparison with RCM simulations. In addition to the 'best estimate' values, daily standard errors (as a measure of interpolation uncertainty) and surface elevation are also provided. The dataset will continue to be maintained and updated beyond the project's duration. As an illustration of the dataset, Figure 8.1 shows the 0.25 degree regular temperature grid for the day with the record high maximum temperature averaged over Europe (30.3°C compared with the 1961–1990 summer mean of 22.4°C). This day was 29 July 2002.

Homogeneity tests by Begert et al. (2008) reveal that many of the underlying station series are subject to potential inhomogeneities (Figure 8.2), for instance as a result of changes in observation practices. This affects, in particular, the understanding of extremes, because changes in extremes are often more sensitive to inhomogeneous climate monitoring practices than changes in the mean. In addition, there are limitations in the ability of the interpolation method to estimate grid values from the underlying station network. Hofstra et al. (2009a, 2009b) found that, in areas where relatively few stations

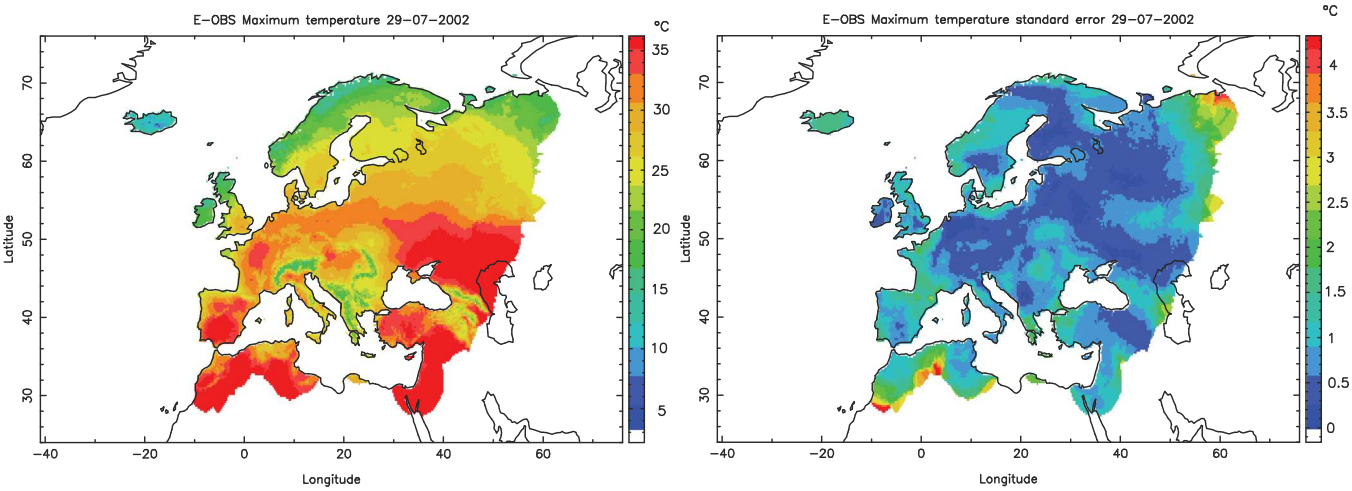

Figure 8.1: Example of E-OBS showing the maximum temperature (left) plus standard error (right) on the hottest day in Europe since 1950: 29 July 2002. The box defines the extent of the dataset. White land areas indicate not enough station data for interpolation.

have been used for the interpolation, both precipitation and temperature are 'oversmoothed'. This leads to reduced interpolated values relative to the 'true' area averages, in particular for extremes. As a result, care has to be taken when using the E-OBS dataset, even though E-OBS is the only daily gridded dataset currently available.

8.4 Representation of key variability phenomena and processes

Systematic errors in the simulation of climate variability have been evaluated by considering whether GCMs are capable of reproducing correctly the intensity, frequency and distribution of the major teleconnection patterns in the tropics and extratropics (such as PNA, ENSO, NAO, Monsoon-Mediterranean, etc.).

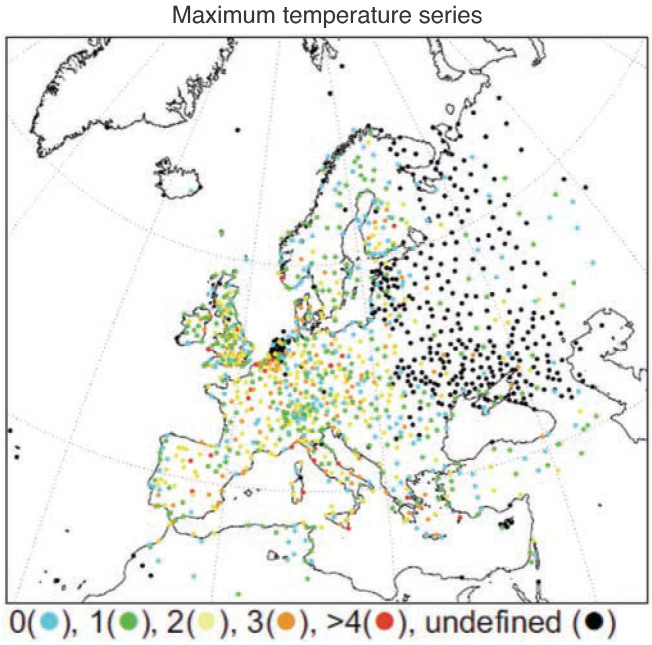

Figure 8.2: Potential number of breakpoints detected using the VERHOM methodology for statistical homogeneity testing of station series (Begert et al., 2008).

The aim was to identify and understand model biases and to provide diagnostics and metrics that help to evaluate aspects of climate models that are critical to assess the response of different models to anthropogenic forcing. This was done firstly by developing diagnostics that were applied to the stream 1 simulations and secondly by sensitivity experiments. The latter serve either to develop new diagnostics or to test the role of particular aspects of model formulation, such as clouds, surface fluxes, or vertical and horizontal resolution. The evaluation focused on the global climate and tropical regions, but tropical–extratropical teleconnections were also considered. Some examples of key phenomena and processes are provided below.

8.4.1 Climate sensitivity and clouds

The analyses of climate sensitivity show that there is a strong relationship between the response of clouds in subsiding regions in the tropics and the magnitude of the temperature change (Dufresne and Bony, 2008; Webb et al., 2006). A first diagnosis (Bony et al., 2006) proposes sorting the atmospheric circulation into convective regimes in the tropical regions. Heat fluxes and cloud radiative forcing can then be compared with satellite data, in a way that clearly identifies the major differences between models that are linked to the convection scheme. In addition, the sensitivity of these fluxes to the SST at the interannual time-scale and the comparison with data has been proposed in order to assess the changes in cloud forcing between different simulations, and to explore the reasons for the range of climate sensitivity found between different models (see also IPCC, 2007).

8.4.2 The east Pacific and the El Niño–Southern Oscillation

The regime-sorted analyses were further extended at a more regional scale to understand the double-ITCZ (Intertropical Convergence Zone) structure produced in most coupled models in the east Pacific (Figure 8.3; Bellucci et al., 2009). The proposed diagnostics show that the double-ITCZ structure results from a too frequent onset of deep convection south of the equator triggered by the convection SST threshold in the models. A major

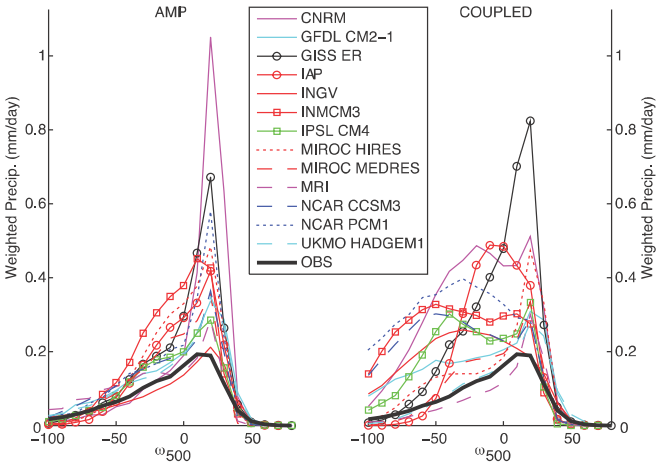

Figure 8.3: Regime-sorted precipitation (mm/day) weighted by the PDF of $^{\omega}500$ for AMIP (left) and the corresponding coupled AR4 models (right) for the region 100 W–150 W, 20 S–0 (Bellucci et al., 2009). Part of the model difference is already found in the atmosphere-only simulation (AMIP), whereas the coupling with the ocean (coupled) and the changes in SST further trigger too deep convection and precipitation, which favour the development of the double-ITCZ structure.

outcome of this work is the identification of two distinct sources for the double-ITCZ error; namely (1) an error in the frequency of the occurrence of deep convection (associated with the ocean–atmosphere coupled interactions), and (2) an error in the magnitude of precipitation for an individual convective event (which can be ascribed to the atmospheric GCM only).

The east Pacific is the core region for the development of the El Niño–Southern Oscillation (ENSO), and the double-ITCZ structure has some implications for the development of the seasonal cycle of SST along the equator and on the characteristics of the interannual variability. The relationship between land and ocean convection has been identified as an important player in the east Pacific, from sensitivity experiments with the IPSL-CM4 coupled model differing only in the convection scheme (Braconnot et al., 2007). Increased resolution is needed to better represent coastal upwelling and the frequency of the Pacific ENSO (Navarra et al., 2008). However a change in model physics (such as convection) has greater implications for model results than a change in resolution. A metric is proposed to characterise the behaviour of ENSO in climate models considering the dynamical and the heat fluxes coupling between the ocean and the atmosphere. Comparing the behaviour of two different convection schemes in the IPSL model, the method clearly shows that the dynamical feedback is underestimated in both versions of the model, whereas the thermodynamic feedback explains why the ENSO has a correct magnitude in one version but is damped in the other version (Guilyardi et al., 2009). This evaluation approach has been extended to all ENSEMBLES stream 1 simulations.

8.4.3 Indian and west Pacific Oceans

Several evaluation studies have considered the Indian Ocean, the west Pacific and the Indian and East Asian monsoon. A diagnostic tool is proposed in order to extract the climatic interannual signals from the non-stationary fields in the simulations and observations. It has been applied to the analyses of the stream 1 simulations. The statistical method allows estimation of the 20th century trends, as well as the relationship between the Indian summer monsoon and the development of ENSO. Relatively cold (warm) SSTs in the central-eastern Pacific are associated with a strong (weak) monsoon during boreal summer in the observations. Results of the analyses show that almost all simulations fail to reproduce this relationship. Sensitivity experiments have been performed to understand the wind-evaporation and the wind-thermocline feedbacks in the east Indian Ocean and to explain why they became a highly significant precursor of ENSO during recent decades. This was done through a sensitivity experiment where SST was altered by ±1°C in the south-east Indian Ocean. The results confirm the important role of this region and the need to reproduce it accurately in climate simulations (Terray and Dominiak, 2005). Specific attention has also been devoted to the modelling of the Asian summer monsoon and the effects of horizontal model resolution, air–sea coupling and improved physics on the simulation of this phenomenon (Alessandri et al., 2007; Cherchi and Navarra, 2007).

Intraseasonal variability (ISV) is also strongly connected with the development of active and break phases of the Indian monsoon. SST warming may affect the characteristics of ISV in the future. A new metric is proposed to assess the representation of the ISV in the climate models. This work was done in close collaboration with the seasonal prediction evaluations to address both the DEMETER and the IPCC class models. The diagnosis uses the local mode analyses proposed by Goulet and Duvel (2000), which was extended by Xavier et al. (2009). The method allows us to detect and to characterise in a simple mathematical form the main events of an intermittent phenomenon. It provides a pattern and statistics for each intraseasonal event that can be combined to assess the simulated ISV with observations. The results show that, for the summer ISV over the Indian Ocean, the DEMETER versions of the climate models produce more reproducible but less realistic ISV patterns compared with the IPCC versions of the models (Figure 8.4). The metric bears a significant relationship with the high frequency variability and the accuracy of the simulated summer monsoon climate. This implies that a correct representation of internal atmospheric processes such as the synoptic weather variability and ISV is required in order to reduce uncertainties in monsoon climate projections (Xavier et al., 2009).

The importance of synoptic weather variability and ISV was further highlighted by analysing the relationship between surface temperature warming over the northern Indian Ocean (the local climate sensitivity) and changes in the strength of the heaviest monsoon rainfall events during boreal summer in climate projections (Turner and Slingo, 2009a,b). This revealed two major subsets among the models: one in which the strengthening of the heaviest monsoon rainfall events is entirely consistent with thermodynamic arguments (the degree of surface warming and available moisture through the Clausius–Clapeyron relation); and another in which the increases include some additional dynamic component. This suggests that the type of convective parameterisation may influence the response of monsoon extremes in the CMIP3 models. Those models with bulk mass-flux-type convection are strongly tied to changes in surface properties and thus have (predominantly) predictable increases

in extremes. Other models, with Arakawa–Schubert type convection, tend to show increases in monsoon extremes far beyond thermodynamic predictions.

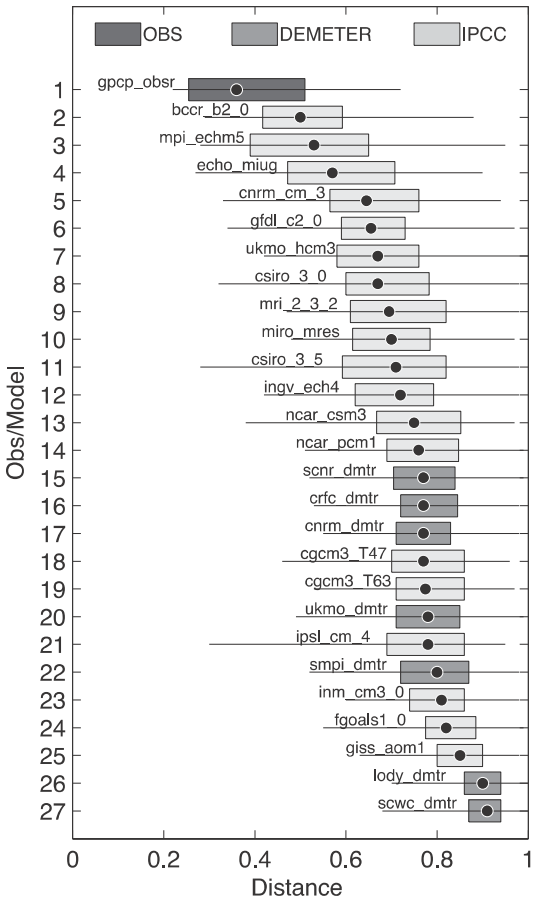

Figure 8.4: Distribution of distances between individual intraseasonal variability (ISV) events to the observed average summer ISV pattern in the observations and models. The bars range from the 25th percentile to the 75th percentile value. The line represents the range of values. The median (50th percentile) values are denoted by the black dots. Models are arranged according to the median distance.

8.4.4 The role of the stratosphere

The effect of systematic biases in the stratosphere on the troposphere climate has been investigated using the ECHAM5 atmospheric model (Giorgetta et al., 2006). The results show how the model representation of the stratosphere has positive effects on the mean state of temperature and wind in the troposphere (Roeckner et al., 2006). It is also shown that these effects are more pronounced when the atmosphere is coupled to the ocean. In addition, changes in the horizontal diffusion scheme are needed, as a direct consequence of the vertical discretisation, to represent properly the dynamics of the stratosphere and the wave-mean flow interaction. These changes affect the Brewer–Dobson circulation as well as the Hadley circulation, and have a positive impact on climate teleconnections between ENSO and the North Atlantic European regions (Cagnazzo and Manzini, 2009). These studies therefore recommend the use of climate models that resolve the stratosphere for climate studies.

8.5 Seasonal to decadal forecast quality

A thorough forecast quality assessment of the seasonal and annual GCM simulations was carried out. Several tools have been made available which help scientists (including those from outside ENSEMBLES) to access and analyse the data. Significant progress has been made with assessing the predictability for the North Atlantic sector and in answering the question why, and under what conditions, a multi-model can outperform the best participating single model.

8.5.1 Forecast quality assessment

A preliminary set of forecast quality results for the seasonal hindcasts over the period 1970–2005 has been published on the website: http://www.ecmwf.int/research/EU_projects/ENSEMBLES. Different aspects of the forecast quality are available for all the single-model systems, as well as for the multi-model. This comparison takes into account the larger ensemble size of the multi-model and thus introduces a reduced multi-model for the comparison with the perturbed-parameter ensemble. A comprehensive assessment of the perturbed-parameter decadal hindcasts suggests that there is a small increase in forecast quality of temperature and precipitation when the predictions are initialised. The increase in forecast quality is found in the first couple of years.

8.5.2 ECMWF seasonal to decadal (s2d) public data server

The capabilities of the ECMWF seasonal–decadal OPeNDAP server have been further enhanced to allow others to perform analyses on the stream 1 seasonal-to-decadal hindcasts. Also, a set of general-purpose forecast-quality assessment tools has been developed for working with the data. In addition, the public data server at ECMWF has been linked to the KNMI Climate Explorer.

8.5.3 KNMI Climate Explorer (http://climexp.knmi.nl)

The KNMI Climate Explorer is a tool which allows anyone to correlate station data, climate indices, observations, reanalysis fields, past seasonal forecasts and climate change experiments. A large number of datasets (both climate model data and observations) have been brought together on a server at KNMI. For the ENSEMBLES project, additional functionality has been added to the Climate Explorer. A set of seasonal forecast verification measures has been added in collaboration with the University of Reading, and links to the seasonal–decadal archive at ECMWF and the RCM archive at DMI have been constructed. As a result, most datasets generated in ENSEMBLES are now also available for analysis in the Climate Explorer. Figure 8.5 illustrates the seamless integration that has been made between the KNMI Climate Explorer and the s2d public data server at ECMWF in a seasonal forecast verification setting.

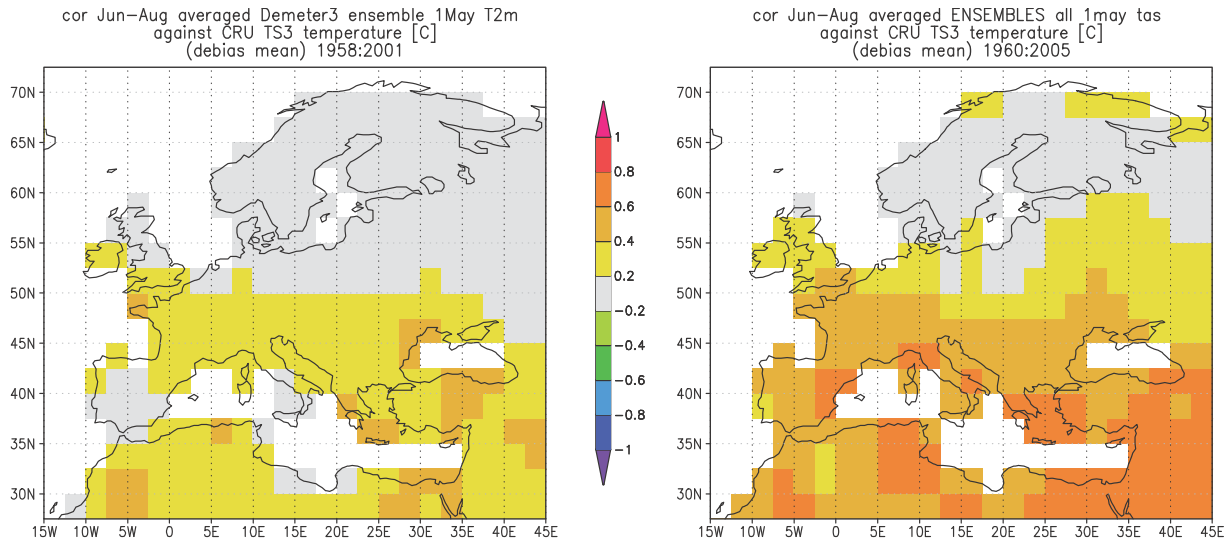

Figure 8.5: Comparison of the point-correlation of summer seasonal predictions of near-surface air temperature started on 1 May of each year against observations for DEMETER (left) and ENSEMBLES stream 2 (right). There is a gain in skill over the Mediterranean area, and over part of Britain; probably as a consequence of the better representation of global warming in the ENSEMBLES experiments. Anybody with internet access can reproduce these plots using the KNMI Climate Explorer linked to the s2d public data server at ECMWF.

8.5.4 North Atlantic sector

Perfect predictability analysis of high-resolution simulations on seasonal to decadal time-scales has been performed for the North Atlantic sector. This focused on assessing the predictability of mid-latitude storms, tropical storms, and weather extremes on these time-scales. Predictability is much higher for the tropical regions, reaching a minimum over central western North America, Greenland and northern Europe.

8.5.5 Mechanics of multi-model combination

Multi-model ensemble combination has become a standard technique to improve ensemble forecasts on all time-scales, including those that are relevant for the ENSEMBLES project. While the success of multi-model combination has been demonstrated in many studies, the underlying mechanisms have so far not been properly understood. The question of why, and under what conditions, a multi-model can outperform the best participating single model has been addressed (Weigel et al., 2008, 2009). The answer is that multi-model ensembles can indeed locally outperform a best-model approach, but only if the single-model ensembles are overconfident (Figure 8.6). The reason is that multi-model combination reduces overconfidence, i.e., ensemble spread is widened while average ensemble-mean error is reduced. This implies a net gain in prediction skill, because probabilistic skill scores penalise overconfidence. Under these conditions, even the addition of an objectively poor model can improve multi-model skill. It seems that simple ensemble inflation methods cannot yield the same skill improvement.

8.6 Extremes in Regional Climate Model simulations

The evaluation of the representation of extremes in RCMs has focused on the European region, with special case studies for the Rhine Basin, the Alps, and the eastern Mediterranean. Both RCM simulations nested within the ERA-40 reanalysis and nested within transient ESM simulations were considered.

8.6.1 Extreme indices in ERA40-driven runs and observations

Maximum (TX) and minimum (TN) temperatures from the CNRM ALADIN RCM simulation were assessed in detail for the Balkan Peninsula using observations from 53 stations (Kostopoulou et al., 2009a). The model performance was first evaluated by calculating the correlation coefficients between the seasonal mean values from the model and the observations. The result for TN is shown in Figure 8.7. The map for the winter season reveals low correlations (<0.4) in the north-western part of the domain in the vicinity of the Dinaric Alps. An area of low

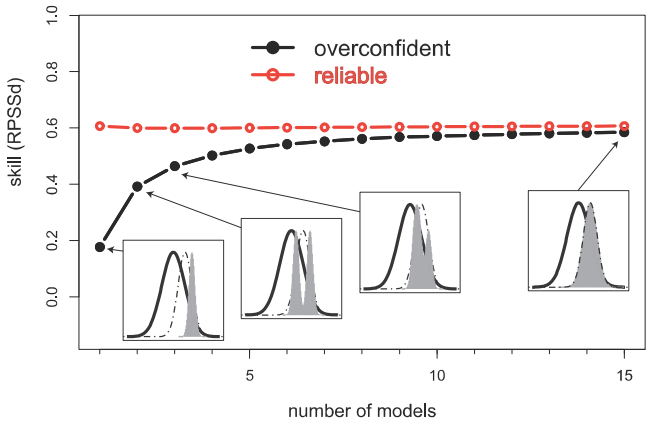

Figure 8.6: Expected skill of multi-model ensemble forecasts as a function of the number of participating single model ensembles. The red line indicates well-calibrated reliable ensembles and the black line represents highly overconfident ensembles. The ensembles have been generated from synthetic toy model simulations. It can be seen that only in the latter case does model combination truly enhance prediction skill, because multi-model combination of overconfident single model ensembles widens the spread. The underlying 'mechanics' of multi-model combination is illustrated by the four small panels at the bottom of the plot: the combination of more and more overconfident single model ensembles (shown as grey shading) successively widens the ensemble spread and reduces the ensemble overconfidence until eventually the entire predictable signal is correctly sampled and forecasts are reliable.

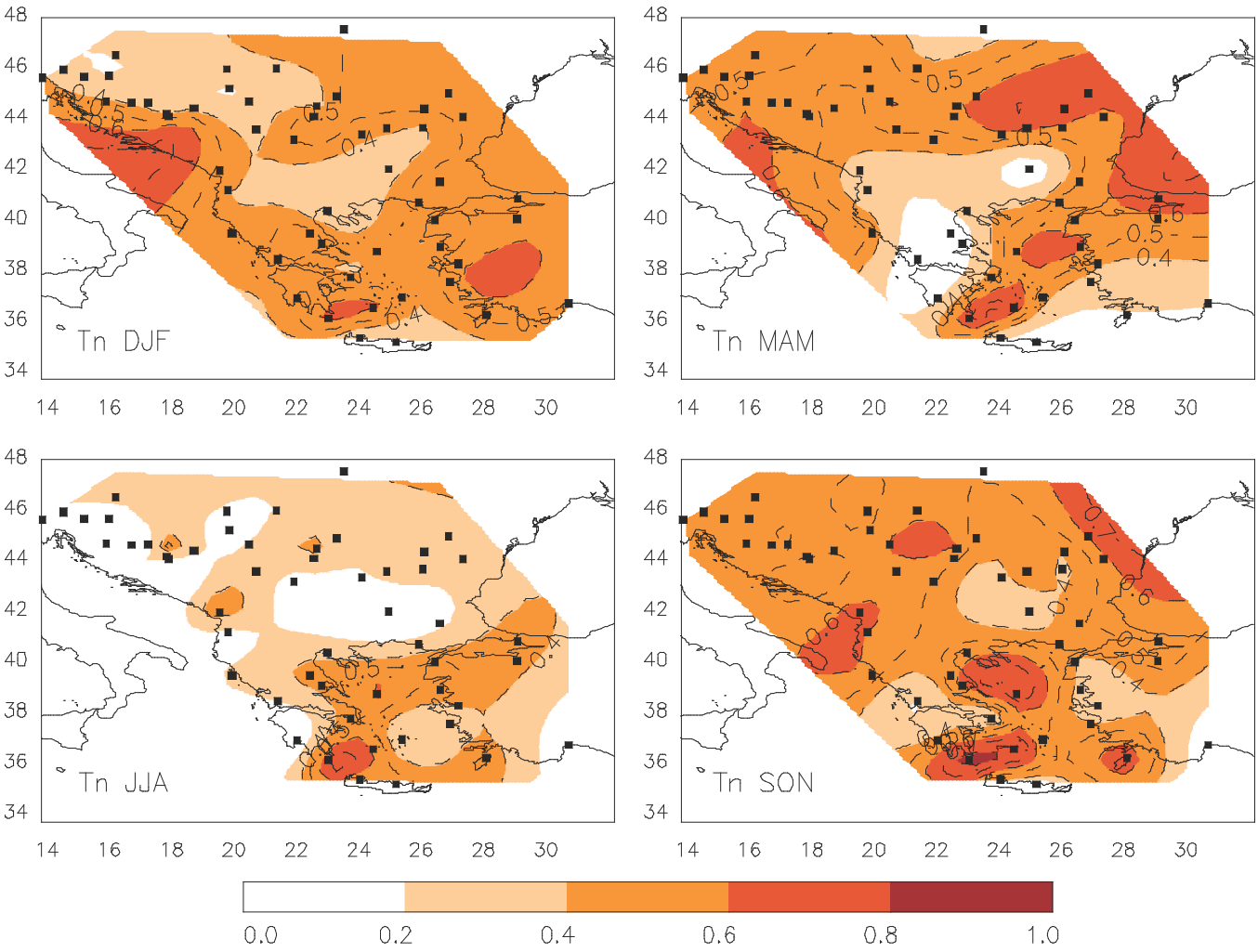

Figure 8.7: Correlations between seasonal mean values of TN from the ERA40-driven CNRM ALADIN RCM simulation and station observations.

correlations is also evident in northern Greece. These low correlations may be attributed to the surface snow scheme of the RCM. In the three other seasons, relatively high correlations are found around the Aegean Sea. Correlations are weak and statistically not significant in summer in the northern part of the domain. A further analysis showed that cold spells (sequences of 5 days or longer below the 10th percentile of TN) were better reproduced than warm spells (sequences of 5 days or longer above the 90th percentile of TX). However, poor results for cold spells were obtained for stations located in the north-western part of the study region, which is consistent with the low correlations in Figure 8.7.

Extreme precipitation events in the Alpine region have been analysed within the ERA40-driven RCM experiments (Pall et al., 2009). Model simulations from fifteen RCMs have been compared to the E-OBS dataset for the baseline 1961–1990 period, using precipitation indices as well as the generalised extreme value (GEV) distribution for estimating return levels of extreme events. Focusing on the 90th percentile of wet days as a simple index of extremes reveals that the models are generally too wet around the southern Alpine rim, and too dry around the Po Valley, though large differences in model performance occur. This is illustrated in Figure 8.8 for autumn, which is climatologically the wettest Alpine season due to moist and weakly stratified southerly airflows (Frei et al., 2006).

8.6.2 Evaluation of trends in extremes in ERA40-driven RCM simulations

Trends in the extremes indices and quantiles of temperatures and precipitation in the ERA40-driven RCM simulations have been compared with those in the E-OBS data for the period 1961–2000 (Lister and Jones, 2009). An example of extreme minimum temperatures is given in Figure 8.9. A salient feature is the strong negative trend in the eastern part of the domain in the autumn season, which is well reproduced by the CHMI-ALADIN RCM simulation. Kostopoulou et al. (2009a) obtained a similar result for the trend in observed extreme minimum temperatures in the autumn season at stations across the Balkan Peninsula and those simulated by the CNRM-ALADIN RCM. By contrast, the RCM simulation in Figure 8.9 is unable to reproduce the trends in the winter extremes in the E-OBS data.

8.6.3 Evaluation of extremes in transient RCM simulations

Hanel and Buishand (2009a) analysed the 1-day summer and 5-day winter precipitation extremes over the Rhine Basin in fifteen RCM simulations (Figure 8.10). For this purpose, the index-flood method has been extended for application to transient climate model simulations (Hanel et al., 2009). The Rhine Basin was

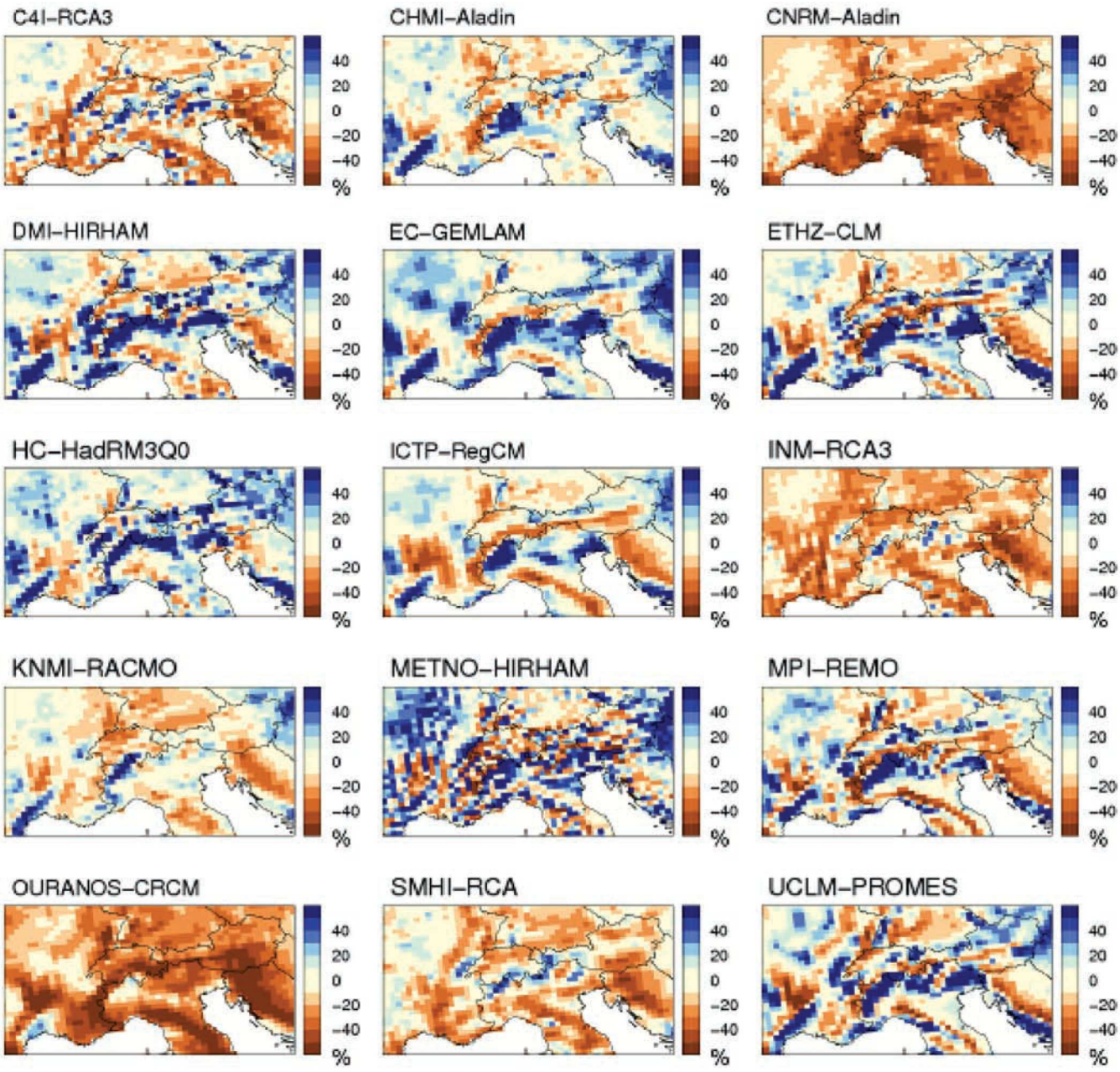

Figure 8.8: Relative bias of the 90th percentile of wet days (>1 mm/day) for all autumn seasons (SON) in the period 1961–1990 (Pall et al., 2009). Shown are the biases in fifteen different ERA40-driven RCMs relative to the E-OBS dataset, on the 0.22 degree (~25 km) rotated grid for the Alpine domain.

divided into five regions. For each region a non-stationary GEV model was fitted. This model assumes that the GEV location parameter varies over the region, while the dispersion coefficient (the ratio between the GEV location and scale parameters) and the shape parameter are constant within the region. All these parameters are allowed to vary with time. Seasonal global temperature anomalies were used as a time-dependent covariate. The estimated GEV parameters for the period 1961–1990 were, for most RCM simulations in the summer season, larger than those from the E-OBS data. These biases could in large part be ascribed to the small number of stations used for gridding the observations. For the winter season, the majority of the RCM simulations considerably overestimated the GEV location parameter and underestimated the dispersion coefficient.

In addition to the model biases, the consistency of projected changes in extremes has also been evaluated. Figure 8.11 shows the projected changes between the periods 1961–1990 and 2070–2099 for the twelve RCM simulations up to the end of the 21st century. Though there is considerable variation in the changes of the extreme value distributions among the RCM simulations, common tendencies can be identified. In the summer season, the dispersion coefficient increases, while there is hardly any change in the location parameter and the shape parameter. As a consequence, there is almost no change in the 2-year quantile, but as the return period gets longer there is a considerable increase due to the increase in the dispersion coefficient. The increase in large quantiles (on average about 15% for the 50-year quantile) is different from the change in mean summer precipitation, which decreases in the majority of the RCM simulations. In the winter season, there is an increase in the location parameter, almost no change in the dispersion coefficient, and a slight decrease in the shape parameter. The increase in the location parameter implies an increase of the quantiles at short return periods. However, the effect of the increase in the location parameter is counterbalanced by the decrease in the shape parameter. As a result there is almost

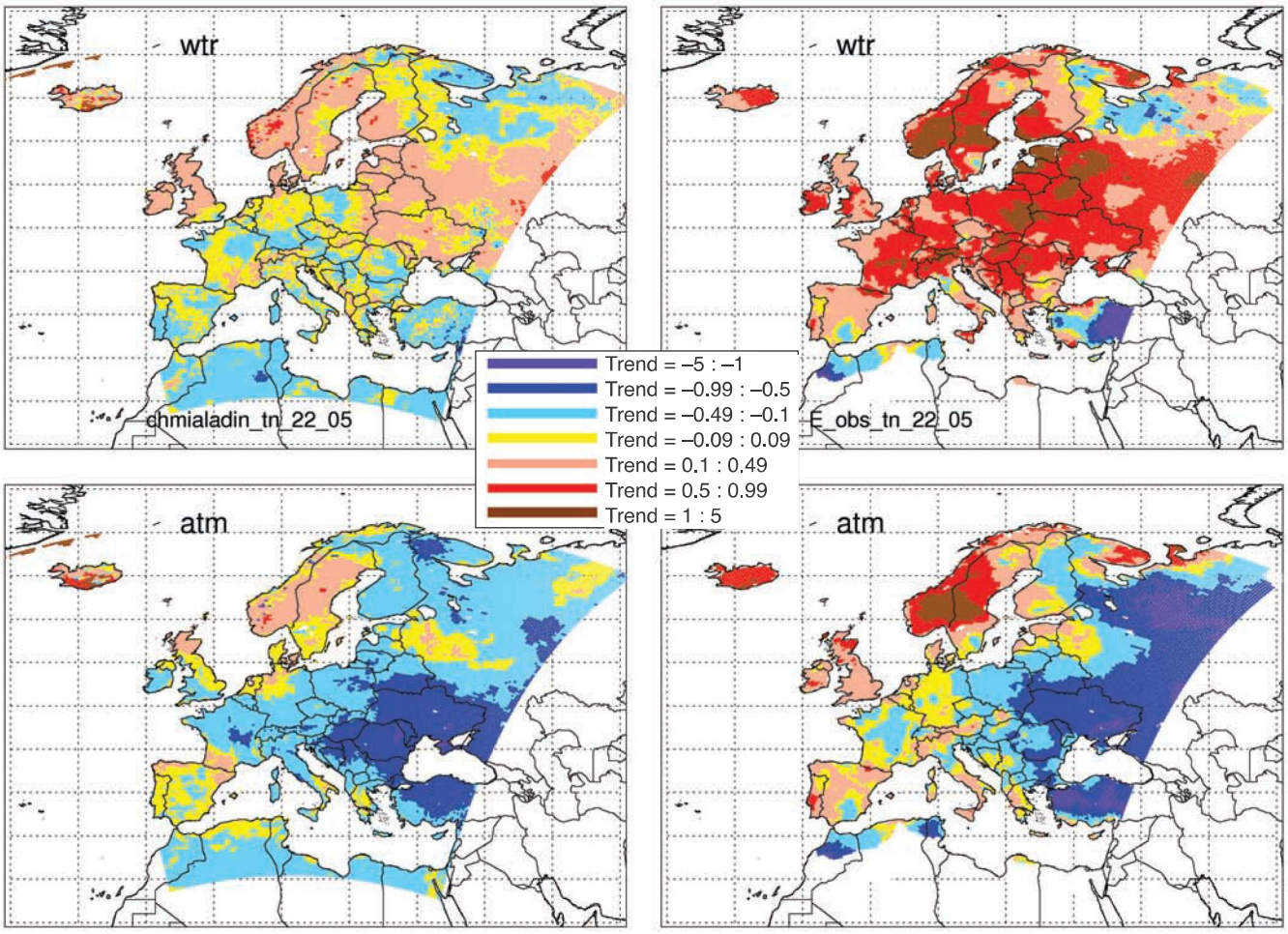

Figure 8.9: Evaluation of trends in extreme minimum temperatures in the period 1961–2000 in the CHMI-ALADIN RCM (Lister and Jones, 2009). The trends (°C per decade) in the 5th percentile of the minimum temperatures (TN05) in the ERA40-driven RCM simulation (left panels) are compared with those in the E-OBS data (right panels) for the winter (upper row) and autumn (lower row) seasons.

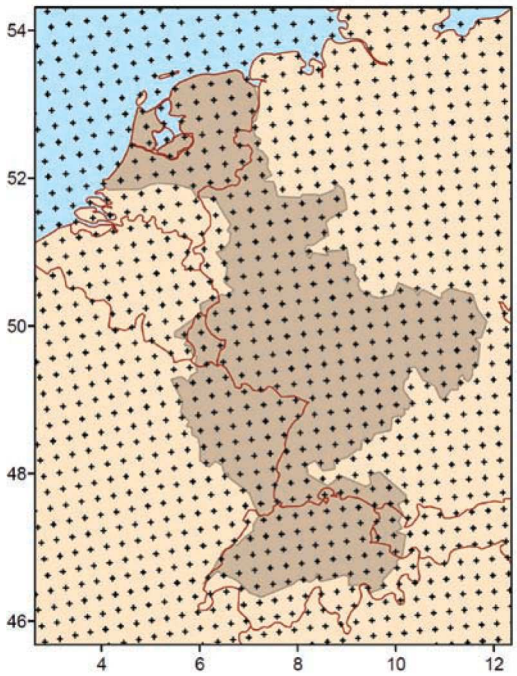

model	acronym	source	period
	— ECHAM5 driven —		
RACMO	**RACMO_EH5**	KNMI	1950-2100
REMO	**REMO_EH5**	MPI	1951-2100
RCA	**RCA_EH5**	SMHI	1951-2100
RegCM	**RegCM_EH5**	ICTP	1951-2100
	— HadCM3Q0, HadCM3Q3, HadCM3Q16 driven —		
HadRM	**HadRM_Q0**	Hadley Centre	1951-2099
CLM	**CLM_Q0**	ETHZ	1951-2099
HadRM	**HadRM_Q3**	Hadley Centre	1951-2099
RCA	**RCA_Q3**	SMHI	1951-2099
HadRM	**HadRM_Q16**	Hadley Centre	1951-2099
RCA	**RCA_Q16**	C4I	1951-2099
	— ARPEGE driven —		
HIRHAM	**HIR_ARP**	DMI	1951-2100
CNRM-RM	**CNRM_ARP**	CNRM	1950-2050
	— BCM driven —		
RCA	**RCA_BCM**	SMHI	1961-2100
HIRHAM	**HIR_BCM**	METNO	1951-2050
	— CGCM driven —		
CRCM	**CRCM_CCC**	OURANOS	1951-2050

Figure 8.10: The Rhine Basin and the RCM simulations with driving ESM used in the study of precipitation extremes in Figure 8.11.

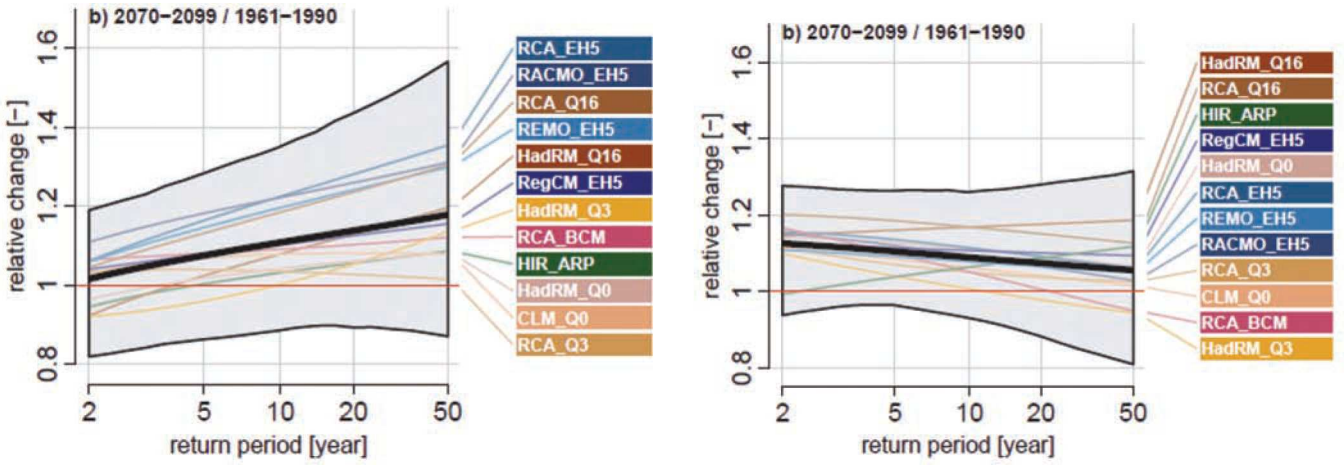

Figure 8.11: Projected changes in precipitation extremes for the Rhine Basin between the periods 1961–1990 and 2070–2099 (Hanel and Buishand, 2009a). Shown are the basin-average relative changes of various quantiles as derived from the changes of the GEV parameters. Left: relative changes in the quantiles of 1-day precipitation maxima in the summer season (JJA). Right: relative changes in the quantiles of 5-day maxima in the winter season (DJF). The thin coloured lines in the figures represent the area-average change for the individual RCMs, the thick black line is the overall mean change. The envelopes indicate the 5th percentile of the minimum and the 95th percentile of the maximum relative basin-average change in 500 bootstrap samples.

no change of large quantiles despite the clear increase in mean winter precipitation in most RCM simulations. The uncertainty of the relative changes in the quantiles, as indicated by the envelope in Figure 8.11, is quite large. This is partly due to the influence of natural variability on the estimated changes.

For the Netherlands, the distributions of the 1-hour and 1-day annual maximum precipitation amounts in eight transient RCM simulations were compared with those from a high-quality radar dataset (Hanel and Buishand, 2009b). The performance of the RCM simulations turned out to be much worse for the hourly precipitation extremes than for the daily extremes. For instance, for the hourly maxima the majority of the RCM simulations underestimate the location parameter by 30–40% with respect to the radar data, whereas the relative bias is no more than 10% for the daily maxima.

Kostopoulou et al. (2009a, 2009b) studied the ability of the ENSEMBLES transient RCM simulations to reproduce extreme climate indices in the eastern Mediterranean region. The evaluation has been initially implemented between the station and the nearest-gridded observed (E-OBS) data at selected sites from the eastern Mediterranean, and then extended to several RCM simulations. The E-OBS dataset satisfactorily reproduced temperature climate indices for most study sites. As expected, the reproduction of precipitation indices was less accurate, in particular for locations with complex topography. Therefore, in some cases it became necessary to use an average of several neighbouring grid points in order to obtain a better representation of the single-site climatic regime. Extreme climate indices were subsequently calculated from ENSEMBLES regional model data and their reliability was assessed against those obtained from the E-OBS dataset. The results varied greatly between sites. In some cases all models performed adequately, while for other sites some models did better than others.

8.6.4 Drought indices

In order to evaluate drought, an optimised objective classification of 'critical dry' circulation patterns (CPs), responsible for major droughts and low river flow periods in south-west Germany has been developed based on fuzzy rules (Bárdossy, 2009). An objective function based upon temporal differences of daily low flows was defined for optimisation purposes. The optimisation was done for different numbers of CPs. Finally, circulation patterns were classified into seventeen classes. Objective CP-MSLP-anomalies have been calculated for the period 1990–1999. These anomalies have been compared with the MSLP anomalies of the so-called 'Grosswetterlagen', which have been discussed in connection with major historical droughts. The objective drought CP anomalies are quite similar to those from the 'Grosswetterlagen'. As an illustration of their usage, maps of a CP-based wetness index have been calculated for 172 grid cells (25 km x 25 km) in the German part of the Rhine Basin for all seventeen CPs. The new CP classification system for droughts has been analysed by observing the occurrence frequencies of the identified critical dry CPs in the study area for historical droughts 1959, 1976, 1991, 2003. In addition, the new drought CPs have been evaluated for RCM simulations (both ERA40- and ESM-driven) for the control period 1960–1991 and the period 2001–2100. For the latter, the A1B scenario runs of RACMO2, REMO and HadRM3 (the standard version as well as the versions with high and low climate sensitivity) were considered. Results for RACMO2 and REMO are very similar, probably due to the same driving ESM (ECHAM5). Frequencies of the combined drought CPs show significant increasing trends for summer for the transient A1B runs of RACMO2 and REMO and do not show any significant change for the three HadRM3 transient runs.

8.7 Quality of impact models

The quality of impact models when forced with downscaled reanalysis data and hindcasts was evaluated through the use of application-specific verification datasets. The evaluation has focused on the seasonal time-scale, considering both Europe and Africa. This work is closely related to RT6. An illustration of the evaluation results is presented below for seasonal forecasts of Malaria. Other results are described in Section 9 together with the impact models.

8.7.1 Malaria forecasts

Seasonal forecast performance was evaluated for malaria prediction in Botswana. The results were obtained by driving the Liverpool malaria model (LMM) with rainfall and temperature forecasts from ENSEMBLES and comparing forecast total malaria incidence for November forecast months 4–6 (February, March and April) with a published malaria index for Botswana for the period 1980–2001 (Figure 8.12; Thomson et al., 2005). A comparison with earlier DEMETER results and with the malaria model driven by 'observations' (ERA-40 reanalysis) has also been made. Overall, the multi-model results for ENSEMBLES show a small improvement from DEMETER, despite a reduction in the number of models from seven to five. Low-malaria events are forecast with the highest skill, although high-malaria events are also forecast skilfully.

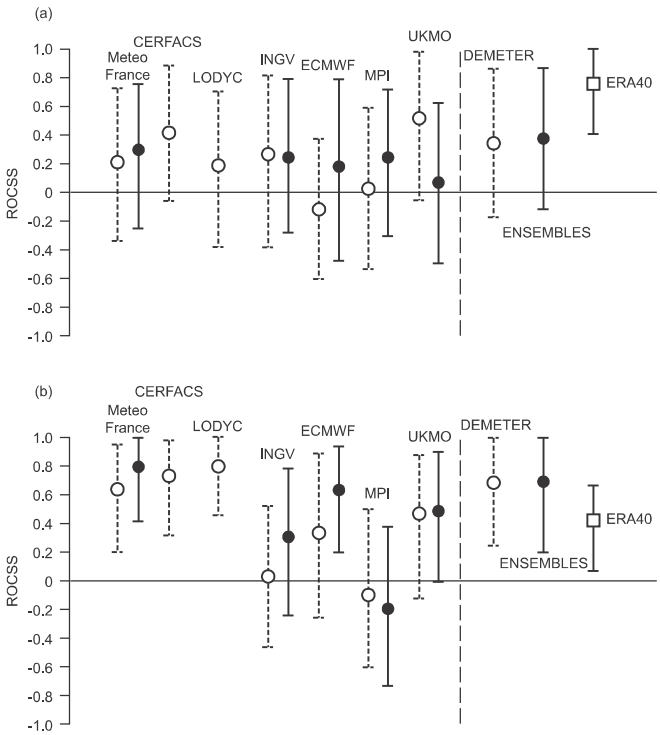

Figure 8.12: ENSEMBLES seasonal forecast performance for malaria prediction in Botswana, for (a) high-malaria events (above the upper tercile) and (b) low-malaria events (below the lower tercile). Single-model results are given on the left of the dashed line, multi-model results on the right. ROC skill score (ROCSS) measures performance relative to climatology: a score of 0 indicates no improvement over a simple climatological forecast. Results were obtained by driving the Liverpool malaria model (LMM) with rainfall and temperature forecasts from ENSEMBLES and comparing forecast total malaria incidence for November forecast months 4–6 (February, March and April) with a published malaria index for Botswana for the period 1980–2001 (Thomson et al., 2005). ENSEMBLES results are shown as solid black circles, with whiskers representing 95% confidence intervals in the ROCSS estimate by 999 bootstrap samples. For comparison, results are also shown for the corresponding model from DEMETER. The hollow squares on the right-hand side show the corresponding scores for the malaria model driven by 'observations' (ERA-40 reanalysis).

References

ENSEMBLES publications are highlighted as bold text.

Alessandri A, Gualdi S, Polcher J, Navarra A, 2007. Effects of land–surface–vegetation on the boreal summer surface climate of a GCM. Journal of Climate 20, 255–278.

Bárdossy A, 2009. Circulation pattern classification and its use in hydrology. Physics and Chemistry of Earth, submitted.

Begert M, Zenkusen E, Häberli C, Appenzeller C, Klok L, 2008. An automated procedure to detect discontinuities: performance assessment and application to a large European climate data set. Meteorologische Zeitschrift 17, 663–672.

Bellucci A, Gualdi S, Navarra A, 2009. The double-ITCZ syndrome in coupled general circulation models: the role of large-scale vertical circulation regimes. Journal of Climate, accepted.

Bony S, Colman R, Kattsov VM, Allan RP, Bretherton CS, Dufresne J-L, Hall A, Hallegatte S, Holland MM, Ingram W, Randall DA, Soden BJ, Tselioudis G, Webb MJ, 2006. How well do we understand and evaluate climate change feedback processes? Journal of Climate 19, 3445–3482.

Braconnot P, Hourdin F, Bony S, Dufresne J-L, Grandpeix JY, Marti O, 2007. Impact of different convective cloud schemes on the simulation of the tropical seasonal cycle in a coupled ocean-atmosphere model. Climate Dynamics 29, 501–520.

Cagnazzo C, Manzini E, 2009. Impact of the stratosphere on the winter tropospheric teleconnections between ENSO and the North Atlantic and European region, Journal of Climate 22, 1223–1238.

Cherchi A, Navarra A, 2007. Sensitivity of the Asian summer monsoon to the horizontal resolution: differences between AMIP-type and coupled model experiments. Climate Dynamics 28, 273–290.

Dufresne J-L, Bony S, 2008. An assessment of the primary sources of spread of global warming estimates from coupled atmosphere–ocean models. Journal of Climate 21, 5135–5144.

Frei C, Schöll R, Fukutome S, Schmidli J, Vidale PL, 2006. Future change of precipitation extremes in Europe: intercomparison of scenarios from regional climate models. Journal of Geophysical Research 111, D06105, doi:10.1029/2005JD005965.

Giorgetta MA, Manzini E, Roeckner E, Esch M, Bengtsson L, 2006. Climatology and forcing of the quasi-biennial oscillation in the MAECHAM5 model. Journal of Climate 19, 3882–3901.

Goulet L, Duvel JP, 2000. A new approach to detect and characterize intermittent atmospheric oscillations: Application to the intraseasonal oscillation. Journal of the Atmospheric Sciences 57, 2397-2416.

Guilyardi E, Braconnot P, Jin F-F, Kim ST, Kolasinski M, Li T, Musat I, 2009. Atmosphere feedbacks during ENSO in a coupled GCM with a modified atmospheric convection scheme. Journal of Climate, doi:10.1175/2009JCLI2815.1.

Hanel M, Buishand TA, 2009a. Evaluation of precipitation extremes in an ensemble of transient regional climate model simulations for the Rhine basin. Climate Dynamics, submitted.

Hanel M, Buishand TA, 2009b. On the value of hourly precipitation extremes in regional climate model simulations. Geophysical Research Letters, submitted.

Hanel M, Buishand TA, Ferro CAT, 2009. A nonstationary index flood model for precipitation extremes in transient regional climate model simulations. Journal of Geophysical Research 114, D15107, doi:10.1029/2009JD011712.

Haylock MR, Hofstra N, Klein Tank AMG, Klok EJ, Jones PD, New M, 2008. A European daily high-resolution gridded dataset of surface temperature and precipitation. Journal of Geophysical Research 113, D20119, doi:10.1029/2008JD10201.

Hofstra N, Haylock MR, New M, Jones PD, Frei C, 2008. Comparison of six methods for the interpolation of daily European climate data. Journal of Geophysical Research 113, D21110, doi:10.1029/2008JD010100.

Hofstra N, Haylock M, New M, Jones PD, 2009a. Testing E-OBS European high-resolution gridded dataset of daily precipitation and surface temperature. Journal of Geophysical Research, doi:10.1029/2009JD011799.

Hofstra N, New M, McSweeney C, 2009b. The influence of interpolation and station network density on the distribution and extreme trends of climate variables in gridded data. Climate Dynamics, in press.

IPCC, 2007. Climate Change 2007: The Physical Science Basis. Contribution of Working Group I to the Fourth Assessment Report of the Intergovernmental Panel on Climate Change (S Solomon, D Qin, M Manning, Z Chen, M Marquis, KB Averyt, M Tignor, HL Miller, eds). Cambridge University Press, Cambridge, UK and New York, 996 pp.

Klok EJ, Klein Tank AMG, 2008. Updated and extended European dataset of daily climate observations. International Journal of Climatology 29, 1182–1191.

Kostopoulou E, Tolika K, Tegoulias I, Giannakopoulos C, Somot S, Anagnostopoulou C, Maheras P, 2009a. Evaluation of a regional climate model using in situ temperature observations over the Balkan Peninsula. Tellus A 61, 357–370.

Kostopoulou E, Giannakopoulos C, Hatzaki M, Founda D, Flocas H, 2009b. On the comparison of extreme climate indices from observed and simulated data in the eastern Mediterranean basin. In: European Geosciences Union General Assembly, Vienna, Austria.

Lister D, Jones PD, 2009. CRU, publication in preparation.

Navarra A, Gualdi S, Masina S, Behera S, Luo J-J, Masson S, Guilyardi E, Delecluse P, Yamagata T, 2008. Atmospheric horizontal resolution affects tropical climate variability in coupled models. Journal of Climate 21, 730–750.

Pall P, Arnold J, Kotlarski S, Bosshard T, Schär C, 2009. Evaluation of heavy Alpine precipitation in ENSEMBLES regional climate models. In preparation.

Roeckner E, Brokopf R, Esch M, Giorgetta M, Hagemann S, Kornblueh L, Manzini E, Schlese U, Schulzweida U, 2006. Sensitivity of simulated climate to horizontal and vertical resolution in the ECHAM5 atmosphere model. Journal of Climate 19, 3771–3791.

Terray P, Dominiak S, 2005. Indian Ocean sea surface temperature and El Niño–Southern Oscillation: a new perspective. Journal of Climate 18, 1351–1368.

Thomson M, Mason S, Phindela T, Connor S, 2005. Use of rainfall and sea surface temperature monitoring for

malaria early warning in Botswana. American Journal of Tropical Medicine and. Hygiene, 73, 214-221.

Turner AG, Slingo JM, 2009a. Uncertainties in future projections of extreme precipitation in the Indian monsoon region. Atmospheric Science Letters 10, 152–158.

Turner AG, Slingo JM, 2009b. Subseasonal extremes of precipitation and active-break cycles of the Indian summer monsoon in a climate change scenario. Quarterly Journal of the Royal Meteorological Society 133, 1143–1157.

Webb MJ, Senior CA, Sexton DMH, Ingram WJ, Williams KD, Ringer MA, McAvaney BJ, Colman R, Soden BJ, Gudgel R, Knutson T, Emori S, Ogura T, Tsushima Y, Andronova N, Li B, Musat I, Bony S, Taylor KE, 2006. On the contribution of local feedback mechanisms to the range of climate sensitivity in two GCM ensembles. Climate Dynamics 27, 17–38.

Weigel AP, Liniger MA, Appenzeller C, 2008. Can multi-model combination really enhance the prediction skill of probabilistic ensemble forecasts? Quarterly Journal of the Royal Meteorological Society 134, 241–260.

Weigel AP, Liniger MA, Appenzeller C, 2009. Seasonal ensemble forecasts: are recalibrated single models better than multimodels? Monthly Weather Review 137, 1460–1479.

Xavier PK, Duvel J-P, Braconnot P, Doblas-Reyes FJ, 2009. An evaluation metric for intraseasonal variability in climate models. Journal of Climate, submitted.